Acta Biomaterialia 8 (2012) 3073–3079

Contents lists available at SciVerse ScienceDirect

Acta Biomaterialia

journal homepage: www.elsevier.com/locate/actabiomat

Electromechanical properties of dried tendon and isoelectrically focused collagen hydrogels

D. Denning [a,b], M.T. Abu-Rub [c], D.I. Zeugolis [c], S. Habelitz [d], A. Pandit [c], A. Fertala [e], B.J. Rodriguez [a,b,*]

[a] Conway Institute of Biomolecular and Biomedical Research, University College Dublin, Belfield, Dublin 4, Ireland
[b] School of Physics, University College Dublin, Belfield, Dublin 4, Ireland
[c] Network of Excellence for Functional Biomaterials, National University of Ireland, Galway, Ireland
[d] Department of Preventive and Restorative Dental Sciences, University of California, 707 Parnassus Avenue, San Francisco, CA 94143-0758, USA
[e] Department of Orthopaedic Surgery, Thomas Jefferson University, 1015 Walnut Street, Philadelphia, PA 19107, USA

ARTICLE INFO

Article history:
Received 17 January 2012
Received in revised form 16 March 2012
Accepted 10 April 2012
Available online 19 April 2012

Keywords:
Atomic force microscopy
Piezoelectricity
Collagen
Isoelectric focusing
Tissue engineering

ABSTRACT

Assembling artificial collagenous tissues with structural, functional, and mechanical properties which mimic natural tissues is of vital importance for many tissue engineering applications. While the electro-mechanical properties of collagen are thought to play a role in, for example, bone formation and remodeling, this functional property has not been adequately addressed in engineered tissues. Here the electro-mechanical properties of rat tail tendon are compared with those of dried isoelectrically focused collagen hydrogels using piezoresponse force microscopy under ambient conditions. In both the natural tissue and the engineered hydrogel D-periodic type I collagen fibrils are observed, which exhibit shear piezoelectricity. While both tissues also exhibit fibrils with parallel orientations, Fourier transform analysis has revealed that the degree of parallel alignment of the fibrils in the tendon is three times that of the dried hydrogel. The results obtained demonstrate that isoelectrically focused collagen has similar structural and electro-mechanical properties to that of tendon, which is relevant for tissue engineering applications.

1. Introduction

Collagenous tissues comprise a major constituent of the extracellular matrix, providing structural support for cells, and performing important developmental and physiological functions [1]. The tissue-specific orientations of collagen fibrils give rise to different functional and mechanical properties [2]. Piezoelectricity is a functional property of collagen, and thus collagen will generate charge under strain (direct piezoelectric effect), and, conversely, undergo deformation in an applied electric field. The direct effect has been linked with the ability of bone to grow and remodel in response to directionally dependent applied stress [3]. Studies of macroscopic electro-mechanical coupling have shown that collagenous tissues such as bone, tendon, dentin, and skin [3–6] all exhibit piezoelectricity. Fibril-forming collagens are composed of collagen molecules, which are hydrogen bond stabilized triple-helical molecules consisting of three polypeptide chains [7]. Collagen molecules have a polar orientation directed from the amino (N)-terminus towards the carboxyl (C)-terminus. Type I collagen molecules self-assemble under appropriate conditions to form fibrils, which maintain the unipolar (N to C) orientation of the monomers at the fibril ends [2]. The staggered stacking of collagen molecules in a fibril gives rise to the characteristic 67 nm D-periodicity, which corresponds to the gap and overlap regions of the molecules, while the cross-sectional hexagonal packing of collagen molecules has been suggested to be the origin of collagen piezoelectricity [5].

Previous studies have demonstrated the potential of collagenous scaffolds [8] and hydrogels [9] for tissue engineering applications [10]. The ability to assemble collagenous scaffolds in vitro with the same structure and properties as natural collagenous tissues would be of significance for studying cell–matrix interactions, as well as for developing compatible engineered tissues. In addition, comparing the electro-mechanical properties between natural collagenous tissues and engineered collagenous constructs could help understand the biological significance of piezoelectricity in collagen. Numerous approaches to assemble fibrillar collagen structures have been implemented, including hydrodynamic flow in the presence of potassium [11,12], magnetic field alignment [13], dip-pen lithography [14], chemical nanopatterning [15], microfluidics [16], and atomic force microscopy (AFM) manipulation [17]. Recent attempts to align collagen by electrochemical processes have demonstrated successful alignment of anisotropically oriented collagen molecules [9,18].

* Corresponding author at: Conway Institute of Biomolecular and Biomedical Research, University College Dublin, Belfield, Dublin 4, Ireland.
E-mail address: brian.rodriguez@ucd.ie (B.J. Rodriguez).

1742-7061/$ - see front matter © 2012 Acta Materialia Inc. Published by Elsevier Ltd. All rights reserved.
http://dx.doi.org/10.1016/j.actbio.2012.04.017

In addition to advantages such as increased mechanical stability [19], aligned collagenous tissues have been shown to influence cell alignment and growth [20].

There are several well-established methods for structural imaging of collagen fibrils and connective tissues, including scanning electron microscopy (SEM) and transmission electron microscopy (TEM) [21,22], however, these techniques require dehydrated specimens and TEM can only provide information on polar order via staining whilst revealing no information on electro-mechanical coupling. AFM allows measurements to be performed in air and liquid, and under physiologically relevant conditions, and recent advances in AFM have contributed to understanding biofunctionality at the nanoscale [23], including nanomechanical mapping of elasticity in mineralized and non-mineralized collagen fibrils [24–26]. Piezoresponse force microscopy (PFM), a technique developed initially to image domains in ferroelectric materials by measuring bias-induced surface deformations [27], has recently been employed to study electro-mechanical coupling in biological systems [28]. PFM is capable of investigating the in-plane and out-of-plane piezoelectric response of biosystems on the nanoscale, including collagen [29–33]. Minary-Jolandan and Yu have observed shear piezoelectricity in single collagen type I fibrils using PFM [31,32]. With PFM not only can fibril alignment be investigated through normal AFM surface topography and deflection images, but the amplitude of the piezoelectric signal and the polarity of the fibrils can be imaged.

Cells have been shown to co-align with aligned collagen fibrils, suggesting that ordered fibrils influence cell polarization [34]. It has also been shown that cells align in the direction of mechanical loading in hydrogels [35], which has been attributed to the triggering of cell surface stretch receptors by mechanical signals. It seems plausible to suggest that such mechanical signals could transform into electrical signals as a result of collagen piezoelectricity. Previous studies have also shown that electrical signals of various strengths and pulses lead to a significant increase in bone cell proliferation [36].

Successfully assembling collagen-rich tissues with similar alignments, orientations, and piezoelectric properties as natural tissues will provide a framework to further our understanding of the role collagen structure and function has on intercellular and cell–matrix communication. The ability to study the piezoelectricity of collagen on the nanoscale will provide a pathway towards understanding mechano-transduction mechanisms and the role electro-mechanics plays in bone remodeling and tissue growth. There may be unidentified benefits of replicating both the functional and structural properties of collagenous tissues. By replicating the phenomenon of electro-mechanical coupling in assembled tissues, the applications of engineered collagen structures can be expanded. Notably, electro-mechanical coupling is a phenomenon exhibited by many biopolymers [3], including chitin, cellulose, poly-L-lysine, which are currently used for biomedical applications [37]. Piezoelectric polymers have also been shown to promote neurite alignment [38]. It is envisioned that not just the structural and chemical properties of such biomaterials should be tailored, but so should the electro-mechanical properties, in order to elicit the desired outcomes for targeted applications.

Here, a comparison of the electro-mechanical properties of isoelectrically focused collagen with rat tail tendon is presented. Rat tail tendon is an excellent tissue for studying collagen as it consists primarily of type I collagen, with only a small volume of proteoglycan, in which the fibrils have a high degree of alignment along the tendon axis [39]. Similarly, isoelectric focusing has been shown to induce the conformational alignment of collagen molecules, which then assemble into hierarchical structures (nano- and microfibrils) that co-align along the axis of the hydrogels [9].

2. Materials and methods

2.1. Preparation of rat tail tendon

Tendon harvested from a rat tail was deposited on gold-coated mica, fixed via carbon tape, and allowed to dry. The tendon fiber used for the study was 440 ± 20 μm in diameter and 4.2 ± 0.02 mm in length, measured using a micrometer. The tendon was bleached in a 4% sodium hypochlorite solution for 20 s in order to partially remove non-collagenous proteins, and thereby expose the fibrils.

2.2. Preparation of isoelectrically focused collagen

Self-assembled, isoelectrically focused collagen hydrogels have been prepared via a method described previously by Abu-Rub et al. [9]. Briefly, a solution of dialyzed type I collagen molecules in 20 nM acetic acid solution was subjected to a d.c. voltage of 3 V at a current of 25 μA in an electro-chemical cell for 60 min. This generates a pH gradient between the electrodes, which causes the collagen molecules to migrate towards their isoelectric point (pH 8). The molecules concentrate and subsequently assemble along this region to form a dense fiber bundle, which is then removed and incubated in polyethylene glycol (PEG)-containing buffer at 37 °C prior to incubation in phosphate-buffered saline (PBS) overnight. The collagen hydrogel is then placed on highly ordered pyrolytic graphite (HOPG) and allowed to dry in air prior to PFM measurements. The dried collagen hydrogel used in the study was 500 ± 20 μm in diameter and 6.50 ± 0.02 mm in length.

2.3. Atomic force microscopy and piezoresponse force microscopy experiments

PFM imaging was performed with an Asylum Research MFP-3D atomic force microscope equipped with a Zurich Instruments HF2LI lock-in amplifier and using conductive MikroMasch DPE18 Pt-coated cantilevers with nominal resonant frequencies and spring constants of 75 kHz and 3.5 N m^{-1}, respectively. The cantilever stiffness is expected to minimize any electrostatic contribution to the measured signal [40]. Prior to imaging, the rat tail tendon and isoelectrically focused collagen samples were placed on a grounded copper plate. During imaging an a.c. signal, $A_0\sin(\omega t)$ (typically 30 V_{rms} at 7 kHz), is applied to the tip, which is in contact with the surface at a constant force (typically 90 nN). The resulting local shear deformations are detected via photodetector signal changes due to cantilever torsion. In this scenario the in-plane polarization is measured, and the technique is typically referred to as lateral PFM (LPFM) [41]. The shear sensitivity was calculated based on the geometry of the cantilever, as described by Peter et al. [42], using the equation, $R = 4L/3h$, where R is the ratio between the in-plane and out-of-plane sensitivities, L is the length of the cantilever (230 μm), and h is the combined height of the tip and cantilever thickness (18 μm). The out-of-plane sensitivity was experimentally measured (53.6 nm V^{-1}), thus the in-plane sensitivity is 913 nm V^{-1}.

The orientation of collagen fibrils exhibiting shear piezoelectricity with respect to the cantilever axis can affect the magnitude of the piezoelectric signal obtained. Thus the sensitivity of the piezoresponse due to the fibril–cantilever geometry must be considered. The maximum detected shear piezoelectric deformation of a single collagen fibril on a substrate due to an applied field occurs when the cantilever axis is perpendicular to the fibril polarization [43]. This geometry also minimizes any contribution of cantilever buckling to the measured lateral signal. High voltage PFM was implemented using a custom built amplifier based on an APEX model

PA85 operational amplifier with a gain of 10, which amplified the a.c. excitation signal. The piezoelectric signal $A_1\sin(\omega t + \Phi)$ resulting from the converse piezoelectric effect and measured via the torsion of the cantilever was demodulated into amplitude (A_1) and phase (Φ) signals using the lock-in amplifier. The acquired PFM amplitude and phase response images indicate the amplitude of the piezoelectric shear deformation and the N to C polarity of the collagen, respectively.

Fibril widths were estimated from the AFM line profiles of 10 fibrils. AFM deflection images are used as individual fibrils are visible in both the dried hydrogel and tendon in these images. For each fibril width reported three line profiles were taken along the length of the fibril to account for any non-uniform fibrillar widths. Only fibrils which were visibly isolated were chosen for analysis.

2.4. Fast Fourier transform analysis

Fast Fourier transform (FFT) analysis (WSxM software [44]) has been used to characterize the alignment of collagen fibrils from both rat tail tendon and isoelectrically focused collagen. FFT analysis of an image converts the information in the image into frequency space. The subsequent FFT output image contains pixels which are distributed in a shape which represents the degree of alignment in the original image. In general, the more symmetrical the shape, the higher the degree of alignment present in the image. Direct comparison of the FFTs from rat tendon and the dried collagen hydrogel is possible using a radial profile plug-in (ImageJ). By summing the pixel intensities along the radius of the circular projection between 0° and 360° in 1° increments the FFT distributions can be visualized and analyzed quantitatively.

3. Results and discussion

3.1. AFM characterization of rat tail tendon and isoelectrically focused collagen hydrogel

The surface properties of rat tail tendon were characterized by AFM. An AFM deflection image of a $5 \times 5\ \mu m^2$ area of the tendon is shown in Fig. 1a. A periodic banding of 67 ± 3 nm is observed, as shown in Fig. 1c, which has been determined by measuring a line profile from 10 fibrils in the image and calculating the average and standard deviation. This periodicity is more readily apparent in the deflection, as opposed to height, images. The fibrils appear to be predominantly oriented along the long axis of the tendon. The average observed fibril width was determined to be 232 ± 35 nm, again calculated from an average of 10 fibrils in the image, which is within the range reported for rat tail tendon (typical fibril diameters are between 50 and 300 nm and vary with the age of the rat [39]).

Fig. 1b shows an AFM deflection image of the dried collagen hydrogel. Several fibrils are aligned along the length of the hydrogel axis, but a considerable number of misaligned fibrils remain. The line profile in Fig. 1d shows the periodic 67 ± 2 nm banding

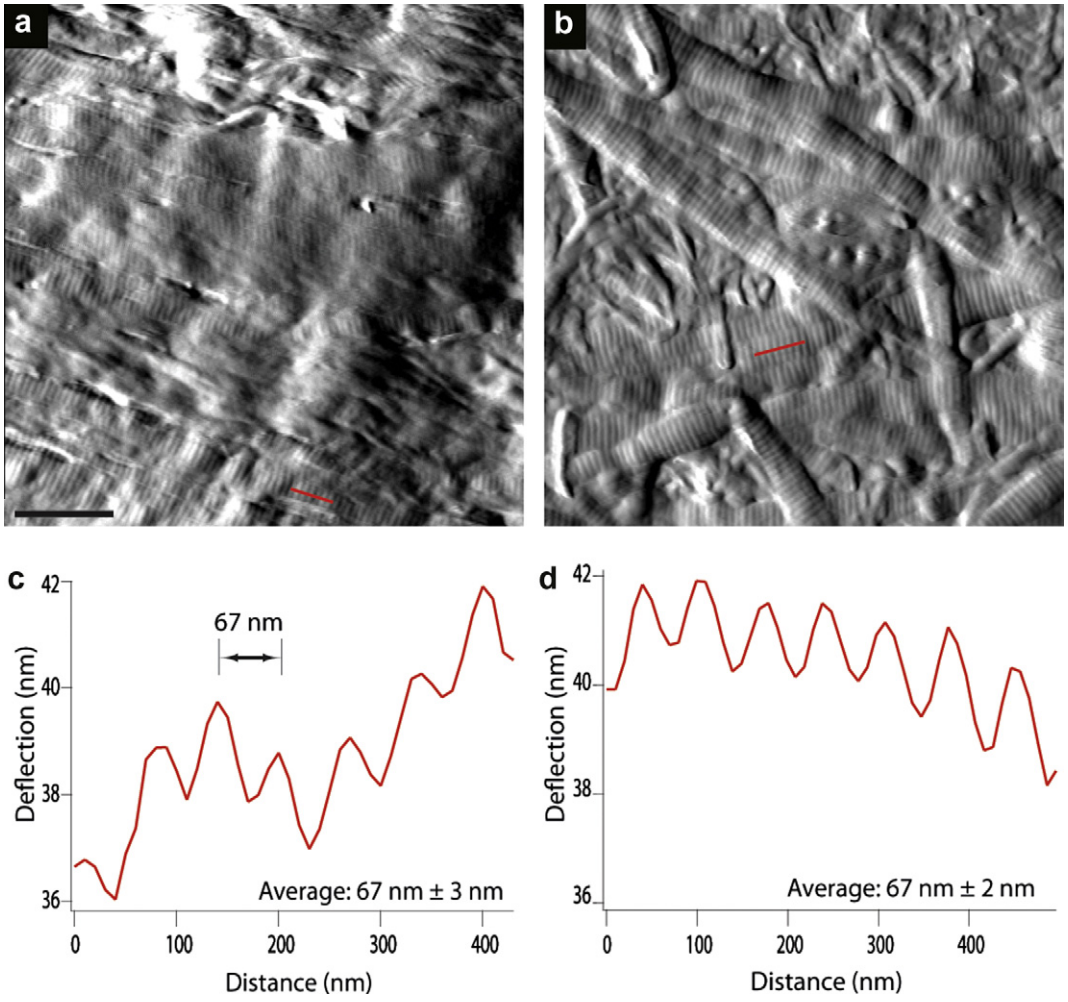

Fig. 1. AFM images of rat tail tendon and the isoelectrically focused hydrogel. (a) AFM deflection image of a rat tail tendon. (b) AFM deflection image of isoelectrically focused collagen. (c) Line profile measured from (a) displaying the periodicity of the collagen fibrils. (d) Line profile measured from (b) confirming collagen periodicity in isoelectrically focused collagen fibrils. Scale bar for (a) and (b) 1 μm.

of collagen and a typical fibril width of 227 ± 46 nm. These results demonstrate the successful replication of fibrillar type I collagen with similar fibril widths. However, from this image we can see that this particular collagen hydrogel does not have the same degree of fibrillar alignment as the rat tail tendon. Note that the PEG buffer stimulates a volume reduction by dehydration, which assists with the fibrillar alignment, thus the tendon and hydrogel samples likely have different water contents and may deform differently during sample preparation.

3.2. PFM characterization of rat tail tendon and isoelectrically focused collagen hydrogel

As collagen is a shear piezoelectric biopolymer [5,29], LPFM has been applied to investigate the in-plane piezoelectric response of the tendon and dried hydrogel. A $20 \times 20\ \mu m^2$ area deflection image of the rat tail tendon is shown in Fig. 2a. At this scan size there is no periodic banding visible. Note that in some regions the tendon may not have been bleached sufficiently to reveal the fibrils. PFM, however, probes a finite volume beneath the tip such that the response of the fibrils underneath can still be visualized [45]. Fig. 2b is the corresponding LPFM amplitude image, which confirms piezoelectricity in the tendon. Each fibril appears to have a constant piezoresponse value along the length of the fibril, and the image illustrates a high degree of alignment of the fibrils. The LPFM phase image (Fig. 2c) displays the N to C polarity, or the polar order, of the collagen fibrils. Since it is non-trivial to identify the polarization direction, a fibril with bright phase contrast (+90°) is assigned as having a N to C polarity pointing to the right of the image, while a fibril with dark phase contrast (−90°) has a polar order pointing to the left. In essence, the fibrils are deforming out of phase with each other during application of the a.c. bias. Note that there is clear evidence of antiparallel polar ordering of the fibrils, whereby adjacent fibrils exhibit polarization in opposite directions. Fig. 2d–f shows LPFM images obtained from a smaller area ($5 \times 5\ \mu m^2$ scan). Collagen fibrils are visible in the deflection image (Fig. 2d), as confirmed by the presence of D-periodicity. The LPFM amplitude image (Fig. 2e) displays a fibrillar level response consistent with the shear piezoelectricity of type I collagen. The average width of the fibrils in the LPFM amplitude image is 200 ± 78 nm. This suggests that the response is due to the piezoelectric activity of individual fibrils, as the average fibrillar widths from the AFM deflection image have been measured to be 232 ± 35 nm. From the LPFM phase image (Fig. 2f) there is further evidence of antiparallel fibrillar ordering along the tendon axis. Comparing the LPFM phase and amplitude images it can be observed that fibrils which exhibit opposite polarization directions undergo equal shear piezoelectric deformations, as expected.

Lateral PFM has been utilized to study electro-mechanical coupling in dried isoelectrically focused collagen hydrogels to compare the shear piezoelectricity of natural and engineered collagen. Fig. 3 shows the LPFM results for the isoelectric collagen. Fibrils are visible throughout the entire deflection image in Fig. 3a. The LPFM amplitude image in Fig. 3b confirms piezoelectricity in the dried hydrogel, suggesting successful replication of this functional property. In the LPFM amplitude image, a higher piezoresponse is observed from fibrils perpendicular to the cantilever and parallel to the scanning direction, which is due to the in-plane shear response of the fibrils and results from torsional twisting of the cantilever. The cantilever–fibril geometry used for all PFM measurements is illustrated in the insets in Figs. 2a and 3a. The long axis of the tendon and dried hydrogel sample is parallel to the scanning direction in all cases. The signal dependence on the angle between the cantilever and fibril is highlighted in Fig. 3e. Fibril 1 has the optimal orientation for measuring the shear response of the fibrils as it is perpendicular to the cantilever and parallel to the scan direction. Fibril 2 displays approximately half of the maximal response as it has a 37° angle with respect to the scan direction. LPFM amplitude

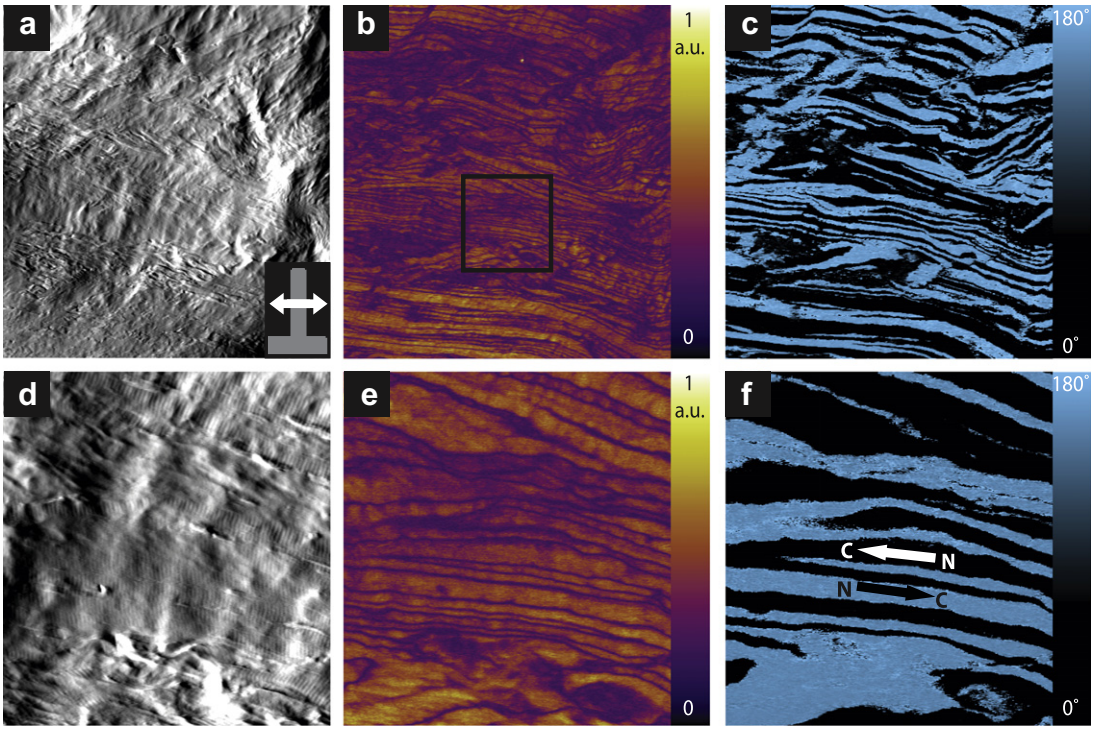

Fig. 2. PFM images of rat tail tendon. (a) AFM deflection image of a rat tail tendon. The inset shows the cantilever orientation and scanning direction (double arrow). (b) LPFM amplitude image measured in the same region as (a). (c) LPFM phase image displaying the polar orientation of the fibrils. Scale bar for (a–c) 5 μm. (d) Smaller scan size AFM image measured from the location indicated by the square in (b), which shows the periodicity of the fibrils. (e) LPFM amplitude and (f) LPFM phase images of the same region as (d). Arrows in (f) indicate the assigned collagen polarity from the N to C termini. Scale bar for (d–f) 1 μm.

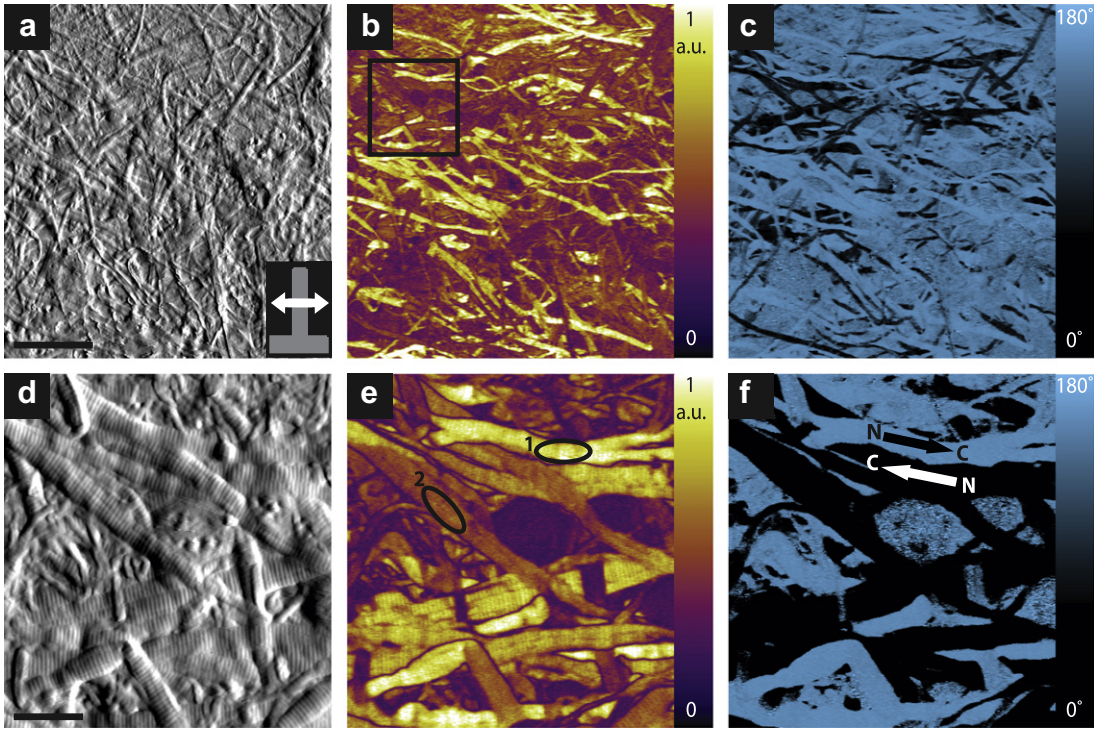

Fig. 3. PFM images of the isoelectrically focused collagen hydrogel. (a) AFM deflection image of isoelectrically focused collagen. The inset shows the cantilever orientation and scanning direction (double arrow). (b) LPFM amplitude image of the same area as (a) and a simultaneously recorded (c) LPFM phase image. Scale bar for (a–c) 5 μm. (d) Smaller scan size AFM deflection image of isoelectrically focused collagen measured from the location indicated by the square in (b). (e) LPFM amplitude and (f) LPFM phase images. The regions circled in (e) show: (1) a fibril aligned with the scan direction; (2) a fibril oriented at an angle with respect to the scan direction. Arrows in (f) indicate the assigned collagen polarity from the N to C termini. Scale bar for (d–f) 1 μm.

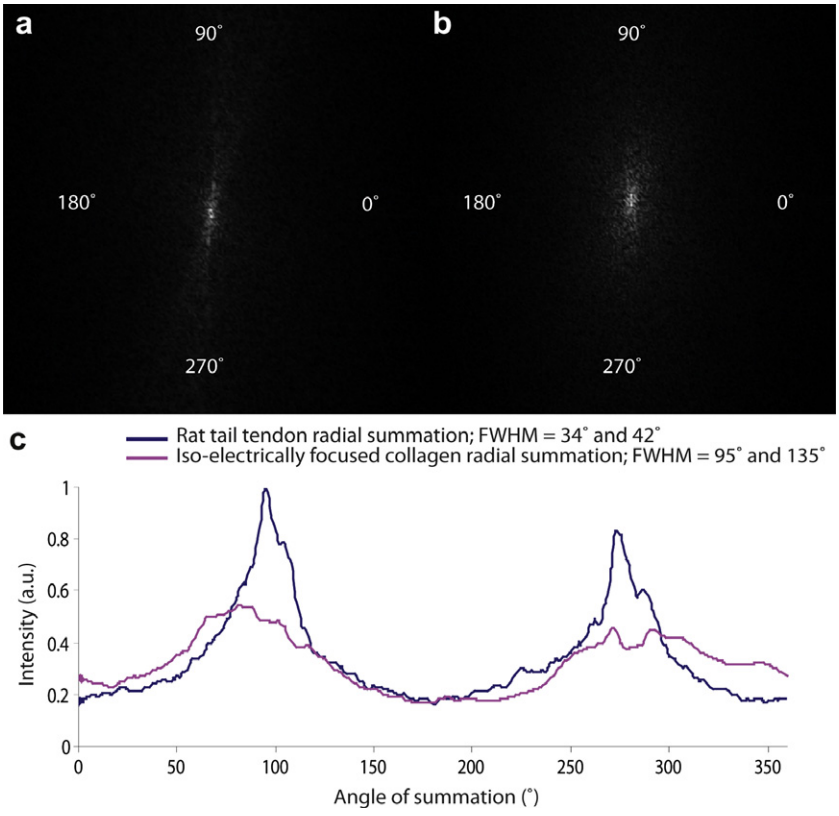

Fig. 4. FFT analysis of rat tail tendon and the isoelectrically focused hydrogel. (a) FFT of the rat tail tendon PFM amplitude image (Fig. 2b) displaying the fibrillar alignment of natural tissue. (b) FFT of the isoelectrically focused collagen PFM amplitude image (Fig. 3b) displaying alignment of grown fibrils. (c) Radial average intensity plot of the rat tail tendon FFT and isoelectrically focused FFT images.

images for rat tail tendon and the dried collagen hydrogel have been normalized to allow direct comparison of the two. The calculated average piezoresponse from the amplitude images measured on both samples indicates that the collagen hydrogel has a 35% higher signal than the tendon. There is also a higher response from fibrils with the optimal orientation (perpendicular to the cantilever) in the dried collagen hydrogel when compared with similar fibrils in the rat tail tendon. This unexpected result may be attributed to incomplete bleaching (Fig. 1a) of the tendon sample or to a change in the tip state, i.e. contamination or coating wear. However, it should also be noted that while the tendon collagen fibrils are cross-linked, there is no specific cross-linking step in the preparation of the hydrogel (non-covalent cross-links are probably present in the hydrogel). This would likely result in a larger piezoelectric signal due to a higher degree of freedom of the molecules, but would require additional study. The LPFM phase image shown in Fig. 3c displays the polar order of the fibrils where a +90° phase is observed for 81% of the image, illustrating that the antiparallel polar ordering observed in the tendon is not replicated in the dried hydrogel.

3.3. Alignment studies of rat tail tendon and isoelectrically focused collagen hydrogel via FFT analysis

Fig. 4 shows the degree of alignment of the fibrils in the tendon. The fibrillar alignment in the tendon and isoelectrically focused collagen has been determined using FFT analysis of the PFM amplitude images and subsequent radial summation of pixel intensities. PFM amplitude images were chosen for the FFT analysis (as opposed to topography images) as the collagen fibrils were not fully exposed in the rat tendon case. FFT and radial averaging analysis of the phase and reconstructed $A_1\sin(\omega t + \Phi)$ images follow the same trend demonstrated by the amplitude images. The FFT of an image containing aligned fibrils will yield an elliptical distribution. The degree of alignment is represented by the full width at half maximum (FWHM) of the peaks obtained from summing the pixel intensities of the FFT image for each degree between 0° and 360°. Fig. 4a shows the FFT of Fig. 2b, which has a narrow peak illustrating alignment of the collagen fibrils in rat tail tendon. Radial summation of the intensity of the rat tail tendon FFT image (Fig. 4c) revealed two peaks at 95° and 275°, indicating strong alignment along the scan direction, and, hence, along the tendon axis. The slight offset from 90° and 270° is due to a slight misalignment of the scan direction with respect to the tendon axis. The FWHM of the peaks were determined to be 34° and 42°, respectively. The radially averaged intensity plots have been normalized using a scaling factor of 3300 to allow direct comparison between the tissues.

The alignment of collagen fibrils in the dried isoelectrically focused collagen hydrogel was also studied using FFT analysis (Fig. 4b). From radial summation of the FFT image (Fig. 4c) there were peaks at 85° and 275°, and the FWHM were measured to be 95° and 135°, respectively. Comparing the average FWHM value for the tendon and dried hydrogel (38° and 115°, respectively), it is apparent that the collagen fibrils in the tendon are three times as well aligned as those in the hydrogel.

4. Conclusion

PFM measurements were performed on both collagen from rat tail tendon and a dried collagen hydrogel formed by isoelectric focusing to study the alignment of both tissues and to investigate their electro-mechanical properties. In the tendon sample the collagen fibrils displayed a high degree of alignment, which is always observed along the length of the long axis of the tendon. LPFM results confirmed fibrillar level shear piezoelectricity in the tendon, and strong evidence of antiparallel polar ordering of neighboring fibrils in rat tail tendon was observed in both large (20 μm) and small (5 μm) scale PFM images. It was shown that the dried collagen hydrogel successfully replicates the characteristic D-period of natural type I fibrillar collagen in tendon. PFM images of the dried collagen hydrogel verify the piezoelectricity of the engineered tissue, demonstrating that isoelectrically focused collagen has similar piezoelectric properties to natural collagen in tendon. The higher piezoresponse signal observed in the dried hydrogel is thought to result from a lack of covalent cross-links present in the engineered tissue. More study is required on the role of covalent cross-links in the piezoelectricity of biosystems. The work presented here has implications for exploiting piezoelectric biopolymers in tissue engineering applications, which may further our understanding of the role of collagen structure and function on intercellular and cell–matrix communication when mimicking, improving, and replacing biological functions.

Acknowledgements

This publication has emanated from research conducted with the financial support of Science Foundation Ireland (SFI10/RFP/MTR2855 and SFI07/SRC/B1163). The authors are grateful for the support of the Nanoscale Function Group and in particular J.I. Kilpatrick and S.H. Loh for building the high voltage amplifier used in this study, and L. Collins and S.A.L. Weber for technical assistance and insightful discussions.

Appendix A. Figures with essential colour discrimination

Figures in this article are difficult to interpret in black and white. The full colour images can be found in the on-line version, at http://dx.doi.org/10.1016/j.actbio.2012.04.017.

References

[1] Fratzl P. Collagen: structure and mechanics. New York: Springer Science+Business Media; 2008.
[2] Prockop DJ, Fertala A. The collagen fibril: the almost crystalline structure. J Struct Biol 1998;122:111–8.
[3] Fukada E. History and recent progress in piezoelectric polymers. UFFC IEEE Trans 2000;47:1277–90.
[4] Marino AA, Becker RO. Piezoelectric effect and growth control in bone. Nature 1970;228:473–4.
[5] Fukada E, Yasuda I. On the piezoelectric effect of bone. J Phys Soc Jpn 1957;12:1158–62.
[6] Marino AA, Gross BD. Piezoelectricity in cementum, dentine and bone. Arch Oral Biol 1989;34:507–9.
[7] Wess T, Hammersley A, Wess L, Miller A. Molecular packing of type I collagen in tendon. J Mol Biol 1998;275:255–67.
[8] Torbet J et al. Orthogonal scaffold of magnetically aligned collagen lamellae for corneal stroma reconstruction. Biomaterials 2007;28:4268–76.
[9] Abu-Rub MT et al. Nano-textured self-assembled aligned collagen hydrogels promote directional neurite guidance and overcome inhibition by myelin associated glycoprotein. Soft Matter 2011;7:2770–81.
[10] Kato YP, Christiansen DL, Hahn RA, Shieh SJ, Goldstein JD, Silver FH. Mechanical properties of collagen fibres: a comparison of reconstituted and rat tail tendon fibres. Biomaterials 1989;10:38–42.
[11] Jiang F, Horber H, Howard J, Muller DJ. Assembly of collagen into microribbons: effects of pH and electrolytes. J Struct Biol 2004;148:268–78.
[12] Loo RW, Goh MC. Potassium ion mediated collagen microfibril assembly on mica. Langmuir 2008;24:13276–8.
[13] Torbet J, Ronzière MC. Magnetic alignment of collagen during self-assembly. Biochem J 1984;219:1057–9.
[14] Wilson DL, Martin R, Hong S, Cronin-Golomb M, Mirkin CA, Kaplan DL. Surface organization and nanopatterning of collagen by dip-pen nanolithography. Proc Natl Acad Sci USA 2001;98:13660–4.
[15] Denis FA, Pallandre A, Nysten B, Jonas AM, Dupont Gillain CC. Alignment and assembly of adsorbed collagen molecules induced by anisotropic chemical nanopatterns. Small 2005;1:984–91.
[16] Lee P, Lin R, Moon J, Lee LP. Microfluidic alignment of collagen fibers for in vitro cell culture. Biomed Microdevices 2006;8:35–41.

[17] Jiang F, Khairy K, Poole K, Howard J, Müller DJ. Creating nanoscopic collagen matrices using atomic force microscopy. Microsc Res Tech 2004;64:435–40.
[18] Cheng X, Gurkan UA, Dehen CJ, Tate MP, Hillhouse HW, Simpson GJ, et al. An electrochemical fabrication process for the assembly of anisotropically oriented collagen bundles. Biomaterials 2008;29:3278–88.
[19] Pins GD, Christiansen DL, Patel R, Silver FH. Self-assembly of collagen fibers. Influence of fibrillar alignment and decorin on mechanical properties. Biophys J 1997;73:2164–72.
[20] Murugan R, Ramakrishna S. Design strategies of tissue engineering scaffolds with controlled fiber orientation. Tissue Eng 2007;13:1845–66.
[21] Birk DE, Hahn RA, Linsenmayer CY, Zycband EI. Characterization of collagen fibril segments from chicken embryo cornea, dermis and tendon. Matrix Biol 1996;15:111–8.
[22] Birk DE, Trelstad RL. Extracellular compartments in tendon morphogenesis: collagen fibril, bundle, and macroaggregate formation. J Cell Biol 1986;103:231–40.
[23] Hansma HG, Hoh JH. Biomolecular imaging with the atomic force microscope. Annu Rev Biophys Biomol Struct 1994;23:115–40.
[24] Wenger MPE, Bozec L, Horton MA, Mesquida P. Mechanical properties of collagen fibrils. Biophys J 2007;93(155):1263.
[25] Balooch M, Habelitz S, Kinney JH, Marshall SJ, Marshall GW. Mechanical properties of mineralized collagen fibrils as influenced by deminerlization. J Struct Biol 2008;162:404–10.
[26] Minary-Jolandan M, Yu MF. Nanomechanical heterogeneity in the gap and overlap regions of type I collagen fibrils with implications for bone heterogeneity. Biomacromolecules 2009;10:2565–70.
[27] Gruverman A, Auciello O, Tokumoto H. Imaging and control of domain structures in ferroelectric thin films via scanning force microscopy. Annu Rev Mater Sci 1998;28:101–23.
[28] Kalinin SV, Rodriguez BJ, Jesse S, Karapetian E, Mirman B, Eliseev EA, et al. Nanoscale electromechanics of ferroelectric and biological systems: a new dimension in scanning probe microscopy. Annu Rev Mater Res 2007;37:189–238.
[29] Halperin C, Mutchnik S, Agronin A, Molotskii M, Urenski P, Salai M, et al. Piezoelectric effect in human bones studied in nanometer scale. Nano Lett 2004;4:1253–6.
[30] Rodriguez BJ et al. Electromechanical imaging of biomaterials by scanning probe microscopy. J Struct Biol 2006;153:151–9.
[31] Minary-Jolandan M, Yu MF. Nanoscale characterization of isolated individual type I collagen fibrils: polarization and piezoelectricity. Nanotechnology 2009;20:085706.
[32] Minary-Jolandan M, Yu MF. Uncovering nanoscale electromechanical heterogeneity in the subfibrillar structure of collagen fibrils responsible for the piezoelectricity of bone. ACS Nano 2009;3:1859–63.
[33] Harnagea C et al. Two-dimensional nanoscale structural and functional imaging in individual collagen type I fibrils. Biophys J 2010;98:3070–7.
[34] Friedrichs J, Taubenberger A, Franz CM, Muller DJ. Cellular remodelling of individual collagen fibrils visualized by time-lapse AFM. J Mol Biol 2007;372:594–607.
[35] Altman G et al. Cell differentiation by mechanical stress. FASEB J 2002;16:270–2.
[36] Brighton CT, Okereke E, Pollack SR, Clark CC. In vitro bone-cell response to a capacitively coupled electrical field. The role of field strength, pulse pattern, and duty cycle. Clin Orthop Relat Res 1992;285:255–62.
[37] Nair LS, Laurencin CT. Biodegradable polymers as biomaterials. Prog Polym Sci 2007;32:762–98.
[38] Lee Y, Collins G, Arinzeh TL. Neurite extension of primary neurons on electrospun piezoelectric scaffolds. Acta Biomater 2011;7:3877–86.
[39] Scott JE, Orford CR, Hughes EW. Proteoglycan–collagen arrangements in developing rat tail tendon. An electron microscopical and biochemical investigation. Biochem J 1981;195:573–81.
[40] Christman JA, Woolcott Jr RR, Kingon AI, Nemanich RJ. Piezoelectric measurements with atomic force microscopy. Appl Phys Lett 1998;73:3851–3.
[41] Abplanalp M, Eng LM, Günter P. Mapping the domain distribution at ferroelectric surfaces by scanning force mircoscopy. Appl Phys A 1998;66:231–4.
[42] Peter F, Rüdiger A, Waser R, Szot K, Reichenberg B. Comparison of in-plane and out-of-plane optical amplification in AFM measurements. Rev Sci Instrum 2005;76:046101.
[43] Sharma P, Wu D, Poddar S, Reece TJ, Ducharme S, Gruverman A. Orientational imaging in polar polymers by piezoresponse force microscopy. J Appl Phys 2011;110:052010.
[44] Horcas I, Fernández R, Gómez-Rodríguez JM, Colchero J, Gómez-Herrero J, Baro AM. WSXM: a software for scanning probe microscopy and a tool for nanotechnology. Rev Sci Instrum 2007;78:013705.
[45] Kalinin SV, Karapetian E, Kachanov M. Nanoelectromechanics of piezoresponse force microscopy. Phys Rev B 2004;70:184101.